Brain Imaging and Behavior (2014) 8:292–299
DOI 10.1007/s11682-013-9254-z

SI: GENETIC NEUROIMAGING IN AGING AND AGE-RELATED DISEASES

Local termination pattern analysis: a tool for comparing white matter morphology

M. Cieslak · S. T. Grafton

Published online: 3 September 2013

Abstract Disconnections between structures in the brain have long been hypothesized to be the mechanism behind numerous disease states and pathological behavioral phenotypes. Advances in diffusion weighted imaging (DWI) provide an opportunity to study white matter, and therefore brain connectivity, in great detail. DWI-based research assesses white matter at two different scales: voxelwise indexes of anisotropy such as fractional anisotropy (FA) are used to compare small units of tissue and network-based methods compare tractography-based models of whole-brain connectivity. We propose a method called local termination pattern analysis (LTPA) that considers information about both local and global brain connectivity simultaneously. LTPA itemizes the subset of streamlines that pass through a small set of white matter voxels. The "local termination pattern" is a vector defined by counts of these streamlines terminating in pairs of cortical regions. To assess the reliability of our method we applied LTPA exhaustively over white matter voxels to produce complete maps of local termination pattern similarity, based on diffusion spectrum imaging (DSI) data from 11 individuals in triplicate. Here we show that local termination patterns from an individual are highly reproducible across the entire brain. We discuss how LTPA can be deployed into a clinical database and used to characterize white matter morphology differences due to disease, developmental or genetic factors.

Keywords DSI· Tractography· Databases· White matter · Individual differences

Introduction

Classical behavioral neurology is rich with descriptions of disconnection syndromes secondary to an impairment of functional integration between different cortical modules due to subcortical lesions (Geschwind and Kaplan 1962). Diffusion-weighted magnetic resonance imaging (DWI) is a popular technique for continuing this research in vivo. DWI samples the diffusion of water molecules along a predetermined set of directions. Myelinated axon bundles in subcortical white matter constrain the directions in which water molecules can diffuse, producing a signal change in the image sampling the direction parallel to the axon bundle's orientation. DWI signal from all the sampled directions is combined to estimate an empirical distribution such as an Orientation Distribution Function (ODF) or to fit a model such as the well-known diffusion tensor used in DTI (Basser and Jones 2002) and quantify directional diffusion anisotropy in each voxel.

These characterizations of diffusivity are typically used to study white matter at two different scales. At the level of a single voxel, a scalar value reflecting the strength of diffusion along a single direction versus all other directions (such as Fractional Anisotropy, FA), is often used as proxy for "white matter integrity" and statistically compared between groups of individuals. At the whole-brain scale, tractography follows the peak diffusion orientations through multiple voxels to reconstruct long-range pathways between distant

This work was supported by the David and Lucile Packard Foundation, PHS Grant NS44393 and the Institute for Collaborative Biotechnologies through contract no. W911NF-09-D-0001 from the U.S. Army Research Office

M. Cieslak (✉) · S. T. Grafton
Department of Psychological and Brain Sciences, UCSB, Santa Barbara, CA, USA
e-mail: matthew.cieslak@psych.ucsb.edu

S. T. Grafton
e-mail: scott.grafton@psych.ucsb.edu

cortical regions (Basser et al. 2000). These pathways, or streamlines, cannot be directly equated to axonal projections, but when combined with high resolution imaging and recent ODF modeling techniques, successfully reproduce known tracts (Fernandez-Miranda et al. 2012). Streamlines are often used to model connectivity between a set of gray matter regions. Both scales of analysis are widely used, but each method has its own set of difficulties.

Voxelwise FA comparisons have been used in a broad spectrum of research projects relating structure, function and performance and are particularly germane for this special issue on the relationship between genetics and white matter organization. Recent studies have examined the consistency of FA values in large twin studies and shown heritability to explain up to 80 % of FA variability in some regions (Chiang et al. 2011). Heritability of DTI FA measures can also be demonstrated in genetically abnormal populations such as Turner syndrome (Yamagata et al. 2012). However, FA comparisons can be difficult to interpret due to some fundamental limitations of the diffusion tensor model (see (Jones et al. 2013) for an instructive review). For example, while low FA may reflect abnormalities in white matter microstructure, it can also be due to normal fiber crossings, partial voluming effects or a number of other non-pathological causes. Higher angular resolution scans and more nuanced models of diffusivity such as HARDI/Q-BALL (Tuch 2004), DSI (Wedeen et al. 2005) and GQI (Yeh et al. 2009) address some of these limitations but are still not as widely used as DTI.

Tractography provides a way to build network models of structural connectivity using streamlines and a discrete set of gray matter regions (Sporns et al. 2005; Bullmore and Bassett 2011). The strength of connectivity between pairs of regions is estimated as a function of the streamlines that terminate within their boundaries. The resulting structural connectivity matrix has become the *defacto* model for the human connectome (Van Essen and Ugurbil 2012). This approach has recently been used to test for genetic influences on network properties such as "global efficiency" in genetically at-risk populations (Shi et al. 2012). Unfortunately, this global parcel and count methodology utilizes a small subset of information about the physical shape of the streamlines, namely the cortical regions in which they terminate. Most of the rich detail available from tractography is lost.

In a recent critique of current DWI methodology, Jones et al. (2013) suggest that for DWI-based connectomics to be more biologically relevant "methods need to be developed that compensate for differences in both length and shape of tracts. Until such time as these methods are developed, it may be dangerous to compare even the streamline count in white matter structures that have different shapes". We propose a new method for analyzing DWI at the local and whole-brain scales simultaneously – in doing so, both the regional connectivity *and* the shape of white matter structures become units of comparison.

Our method is based on an intuition commonly used when checking tractography results. Tractography visualization tools such as trackvis (Wang et al. 2007) typically support a "sphere dissection" feature, where the user can move a sphere through space while the software renders the sphere and all streamlines passing through it in a 3D viewer. With a quick sphere placement the user can, for example, check that a sphere placed in the internal capsule streamlines connecting primary motor cortex to the brainstem. We have encapsulated this notion – of selecting only streamlines passing through a local neighborhood of voxels and examining their endpoints – into an algorithm called local termination pattern analysis (LTPA, Fig. 1).

LTPA operates on spatially normalized tractography datasets from multiple individuals. A *search sphere* is defined around a coordinate in white matter and all streamlines intersecting this sphere are collected (Fig. 2a). These streamlines and the pairs of gray matter regions they connect are used to construct a streamline *termination pattern* for each individual. Termination patterns are N element vectors where N is the total number of unique region pairs connected by streamlines passing through the search sphere across all individuals. It is essentially the flattened upper triangle of a structural connectivity matrix (Fig. 2b). With termination patterns for each individual in hand, a number of techniques may be applied depending on the research question. If the goal is to contrast a group of individuals with a specific neurological condition to a group of healthy individuals, a machine-learning analysis can be performed to see if termination patterns are separable between groups. The correlation between genes and the presence or absence of a connection passing through the search sphere can be computed. In the present study, we compute the correlation coefficients of termination patterns within and between individuals to demonstrate the robustness of our method. Regardless of the analysis chosen, the procedure is repeated for spheres centered on every voxel in white matter. Results of each comparison are saved in the central voxel of each sphere, producing an *LTPA map* much like the "information map" produced by the fMRI searchlight method (Kriegeskorte 2006). It is therefore possible to produce an LTPA correlation map (Fig. 3), an LTPA GWAS map or an LTPA classification accuracy map.

LTPA mapping has two noteworthy properties. Suppose a classifier is used in each sphere to distinguish between two groups of individuals. Due to the geometric properties of searching a space with a fixed-size sphere as the structuring element, differences in local termination patterns between two groups will appear in the LTPA map as a cluster of high classifier accuracies proportional in size to the radius

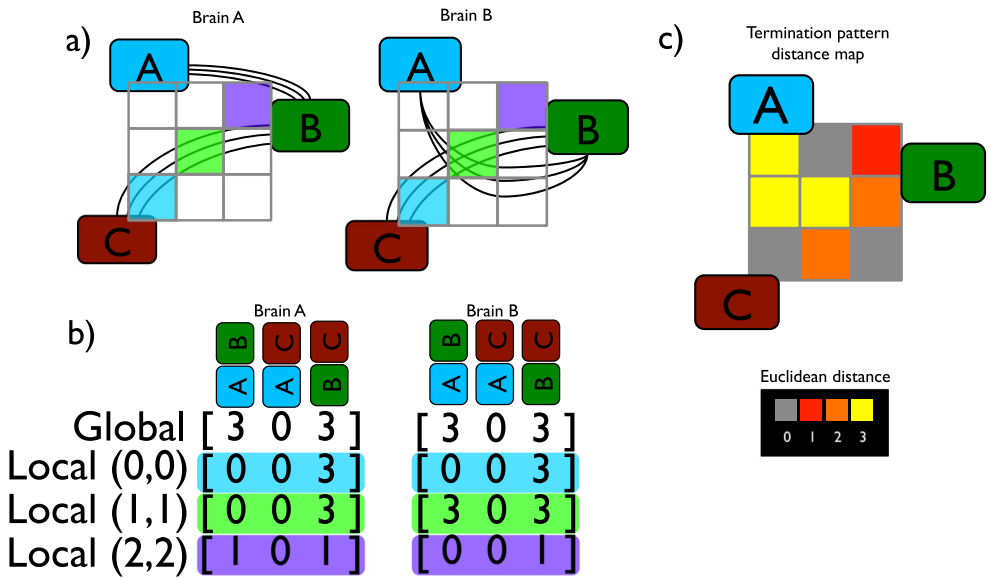

Fig. 1 A schematic of LTPA for comparing two brains. **a** Assume that there are three structures in the brain named A,B and C. We scan two individuals and tractography reconstructs 6 streamlines in each brain. **b** The conventional network approach is taken and a whole-brain connectivity matrix is estimated (similar to Hagmann et al. 2007; Bassett et al. 2011). This matrix is converted to a vector, producing the "Global" termination pattern in Fig. 2b. In this case the network approach reveals no difference between the two brains. Instead, we use LTPA to map local termination pattern differences at three "voxels" by computing Euclidean distance. The location at the cyan voxel observes no difference, at the green a large difference and at the purple a subtle difference. **c** Local termination patterns are compared at each voxel using Euclidean distance and the distance value is mapped back to the brain. The map reveals differences in the voxels where the A to B connection has a different shape

of the search sphere (Viswanathan et al. 2012). If a bundle of streamlines is present in one group and missing in the other, all search spheres falling in the path of that bundle will show high classification accuracy. This appears in the LTPA accuracy map as a cluster of high classification accuracies in the shape of the missing bundle. Secondly, if both groups have statistically indistinguishable whole-brain connectivity matrices but the shape of a connection differs, the voxels where the shapes differ will show high classification accuracy (Fig. 1c).

Local termination pattern analysis can be used as a complimentary tool for whole-brain connectivity comparisons based on age, gender, disease state, genetics or any other systematically varying factor. However, before the method can be applied in a research setting to assess differences between individuals or groups, we must show that termination patterns are a reliable unit for comparison. To this end, we scanned 11 individuals in triplicate and measured the reproducibility of termination patterns both within and between subjects. Due to the effects of atlas choice (Zalesky et al. 2010; Hagmann et al. 2010) on brain connectivity estimates and the known effects of search sphere size in traditional searchlight analyses (Viswanathan et al. 2012), we assessed termination pattern reproducibility at two different atlas resolutions using two different sphere radii.

Methods

Data acquisition and preprocessing

Diffusion spectrum images (DSI, Wedeen et al. (2005)) were acquired for a total of 11 subjects in triplicate (mean age 27 ± 5 years, 2 female, 2 left handed) along with a T1 weighted anatomical scan at each scanning session. DSI scans sampled 257 directions using a Q5 half shell acquisition scheme with a maximum b value of 5000 and an isotropic voxel size of 2.4mm (Axial acquisition, TR = 11.4s, TE = 138ms, 51 slices, FoV (231,231,123 mm)).

DSI data were reconstructed in DSI Studio (www.dsi-studio.labsolver.org) using q-space diffeomorphic reconstruction (QSDR) (Yeh and Tseng 2011). QSDR first reconstructs diffusion weighted images in native space and computes the quantitative anisotropy (QA) in each voxel. These QA values are used to warp the brain to a template QA volume in MNI space using the SPM nonlinear registration algorithm. Once in MNI space, spin density functions were again reconstructed with a mean diffusion distance of 1.25mm using three fiber orientations per voxel. Fiber tracking was performed in DSI Studio with an angular cutoff of 55°, step size of 1.0mm, minimum length of 10mm, smoothing of 0.0, maximum length of 400mm and a QA

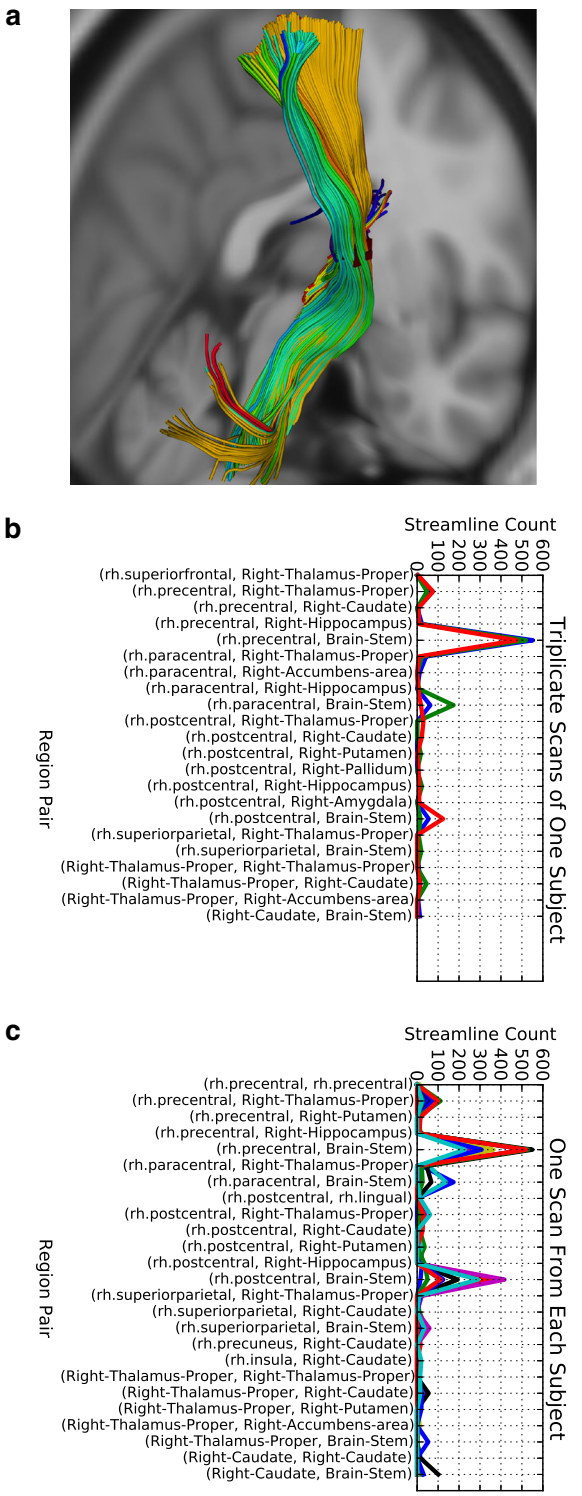

Fig. 2 **a** An example "sphere dissection". Voxels in the search sphere are colored dark red. Streamlines intersecting these voxels are collected from one subject and rendered. The color of each streamline is determined by the pair of structures it connects. **b** Local termination patterns generated by the search sphere in (**a**) are plotted for three separate scans of the same individual. The mean correlation coefficient is $\bar{r} = 0.95 \pm 0.03$. **c** Local termination patterns of one scan from each subject are plotted. The mean correlation coefficient between subjects is $\bar{r} = 0.84 \pm 0.13$

threshold determined by DWI signal in the CSF. Deterministic fiber tracking using a modified FACT algorithm was performed until 100,000 streamlines were reconstructed for each individual.

Anatomical scans were segmented using FreeSurfer (Dale et al. 1999) and parcellated according to the Lausanne 2008 atlas included in the connectome mapping toolkit (Gerhard et al. 2011; Hagmann et al. 2008). Two parcellation schemes, scale 33 (containing 83 regions) and scale 60 (129 regions) were registered to the B0 volume from each subject's DSI data. The B0 to MNI voxel mapping produced via QSDR was used to map region labels from native space to MNI coordinates. To extend region labels through the gray/white matter interface, both atlases were dilated by 4mm. Dilation was accomplished by filling non-labeled voxels with the statistical mode of their neighbors' labels. In the event of a tie, one of the modes was arbitrarily selected. Each streamline was labeled according to its terminal region pair, one label for each of the Lausanne atlases.

Discrete space indexing and local termination pattern analysis

Once in 2mm MNI space, a hash table h was generated for each subject where each coordinate $c_n = (i, j, k)$ is mapped to a set of tuples containing streamline id numbers, endpoint labels and their array of coordinates: $h(i, j, k) \rightarrow \{(\mathrm{id}_1, \mathrm{label}_1, \mathrm{X}_1), \ldots\}$. A search is conducted with a center coordinate c and a radius r. Parameters c,r are used to construct a set of coordinates $C = \{c_1, c_2, \ldots c_n\}$ such that c is the center and all other voxels are within r millimeters of c. Querying h with C returns a set of streamlines $S = h(c_1) \cup h(c_2) \cup \cdots \cup h(c_n) \forall c_i \in C$. This formulation prevents double-counting of streamlines passing through multiple voxels in the search sphere. Figure 2a depicts a query in the corticospinal tract. $C(r = 2, c = (33, 54, 45))$ is rendered as a set of red cubes. S is plotted such that each streamline X is colored based on its label, not its orientation in space. In this case, the label was determined by the streamline's termination regions in the Lausanne scale 33 atlas.

Termination patterns are defined by counts of each streamline label in S. One termination pattern is computed for each scan. Connections where no streamlines were observed in any subject were not included as elements in the termination pattern.

Results

Figure 2b shows termination patterns returned from three separate scans of the same subject. Figure 2c plots termination patterns from a single scan of each subject. In

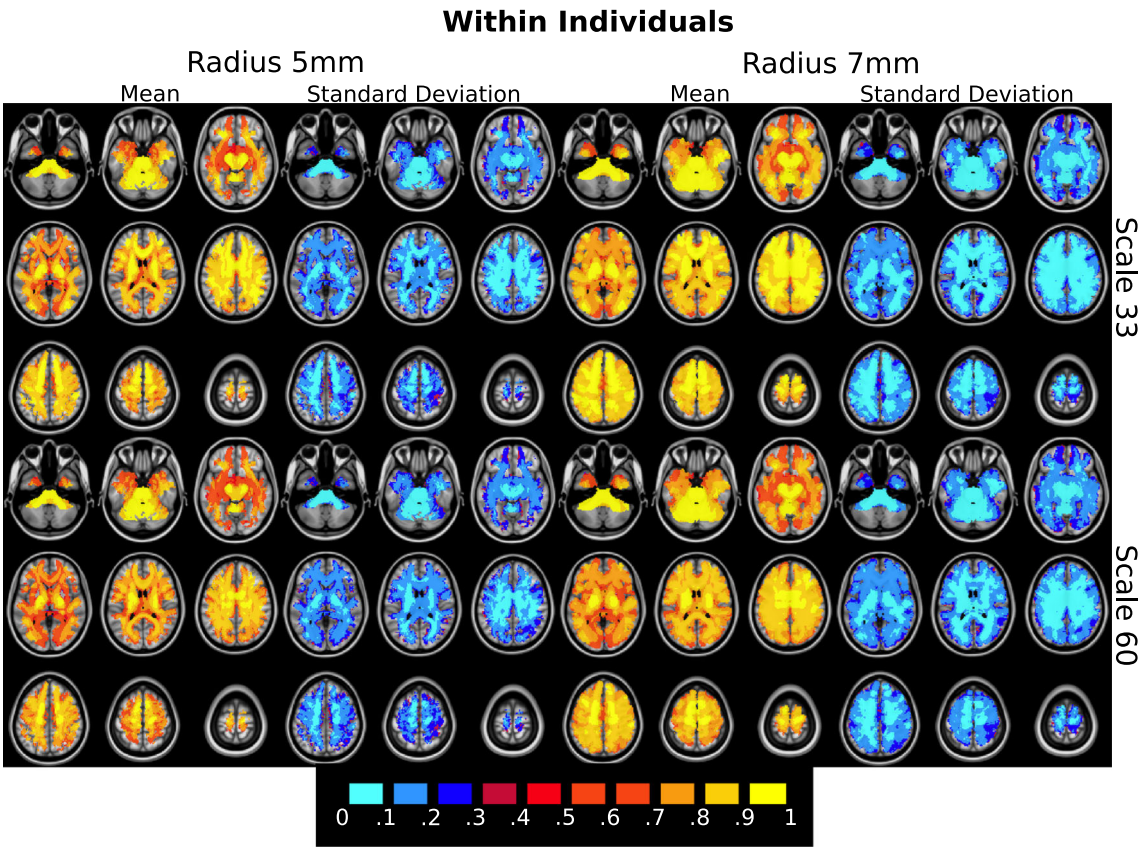

Fig. 3 A summary of the distributions of within-subject correlation coefficients. Columns display the mean or standard deviation of within-subject correlation coefficients for search spheres of 5mm radius (*left columns*) and radius 7mm (*right columns*). Distributions displayed in the top row were observed when using the scale 33 atlas, the bottom row using scale 60. Search spheres around colored voxels produced mean correlation coefficients significantly higher than those observed when permuting streamline counts

each sphere, local termination patterns were combined to form L, a 33-by-M matrix where rows contain the counts of streamlines connecting each of the M observed region pairs for each the 33 scans. To establish the reproducibility of termination patterns, we calculated Pearson's correlation coefficient between all pairs of rows in L. These coefficients were split into two categories. If the correlation was calculated between two scans of the same individual, this value is a *within-subject* correlation coefficient. Correlation coefficients between two scans from different subjects are *between-subjects*. Complete pairwise comparisons in our data produces 33 within-subject and 495 between-subject correlation coefficients.

Both within and between-subjects correlation coefficient means were tested for significance using a permutation test. Streamline counts in the local termination patterns of each subject were shuffled and used to compute within and between-subject correlation coefficient means 100 times in each sphere. Separate sampling distributions were constructed for within and between subject means to account for their different sample sizes. The actual correlation coefficient means were compared to their corresponding sampling distributions to obtain a p-value. Colored voxels in Figs. 3 and 4 reflect spheres where the observed correlation coefficient means are greater than all 100 permutations ($p < 0.01$).

The distribution of the 33 within-subject correlation coefficients reflects the reliability of local terminations from the same individual. Values close to 1 indicate that local termination patterns are not corrupted by errors in ODF reconstruction or tractography. Values close to 0 indicate that LTPA in this sphere would not be suitable for making inferences about white matter structure. Figure 3 displays the mean within-subject correlation coefficients in each sphere. These values vary depending on the radius of the search sphere and the spatial resolution of the atlas used to define regions. However, within-subject correlation coefficients were significantly greater than 0 across most of white matter regardless of search sphere radius or atlas resolution.

The distribution of the 495 between-subject correlation coefficients, assuming the within-subject correlations are high, reflect the similarity of local termination patterns

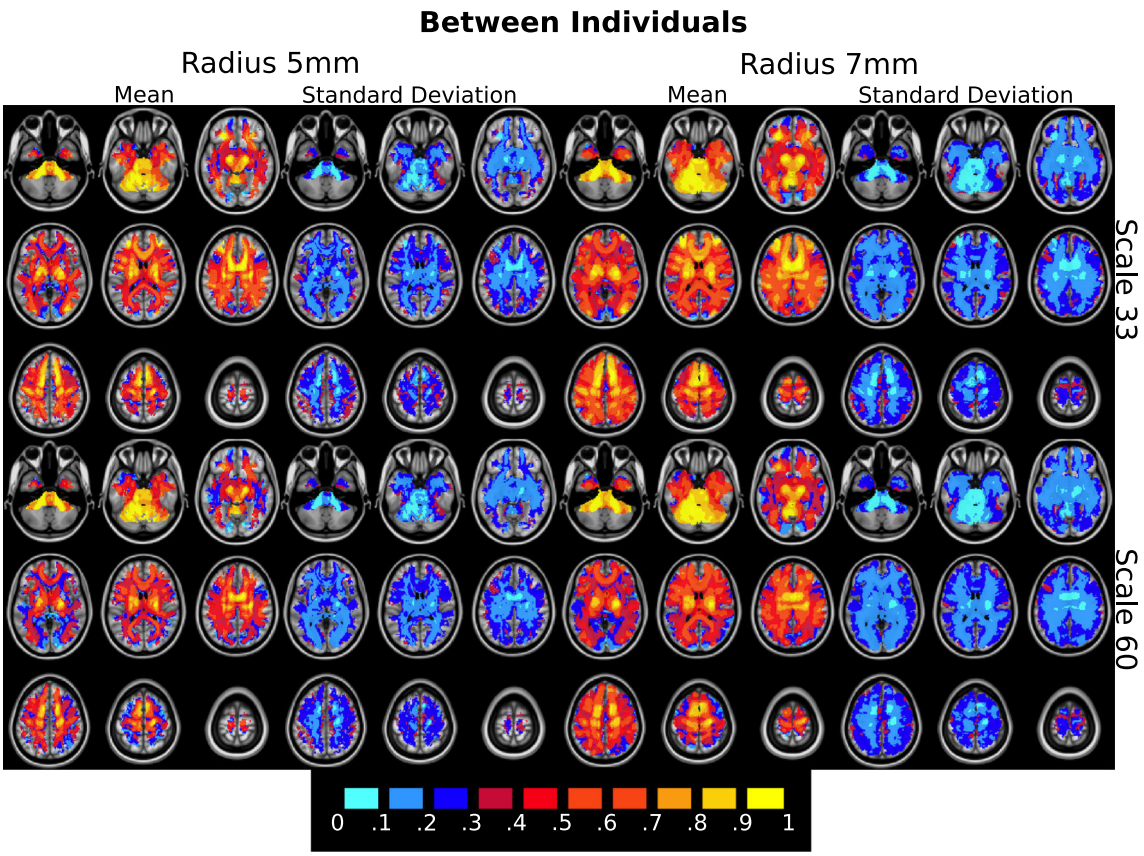

Fig. 4 The same mapping parameters are used as in Fig. 3, but here the between-subjects correlation coefficient distributions are described

across individuals. Maps in Fig. 4 show that between-subject correlations are high along large white matter tracts, indicating that these structures produce highly consistent local termination patterns. Correlations are well over .6 in the corticospinal tract, longitudinal fasciculi and genu of the corpus callosum. Low between-subject together with high within-subject correlations near the gray/white matter interface suggest these areas are rich source of individual anatomical variability.

A similar within/between subject correlation approach has been used previously to characterize the reproducibility of whole brain structural connectivity matrices (Cammoun et al. 2012). Each voxel in a Figs. 3 and 4 could be thought of as Cammoun et al.'s whole-brain graph reliability measure evaluated on all possible subgraphs, each conditioned on the streamlines constituting their edges pass through that voxel's neighbors.

Discussion

Extensive collections of clinical DWI data can produce large databases of tractography information. LTPA, combined with technology for storing and retrieving big data, may be an ideal approach to exploring white matter structures. The process of searching a set of spatial coordinates, collecting region pair labels from intersecting streamlines and consolidating them into termination patterns translates easily into a Map/Reduce problem. A number of technologies including MongoDB (www.mongodb.org) and Hadoop (hadoop.apache.org,) implement Map/Reduce on a large scale, providing the benefits of distributed computing and potentially supporting a web interface accessible to other researchers. LTPA on a smaller scale can be run on a typical desktop computer. Our present implementation of LTPA uses python dictionary objects to implement the mapping h from spatial coordinates to streamline ID's. Similar functionality has recently been included in DiPy (Garyfallidis et al. 2011).

It is important to note that in this study we used LTPA to map termination pattern *similarity* across subjects. The fact that within-subject similarity is much higher than between subject similarity is also a comforting reassurance that similarity is not simply being driven by consistent artifacts in reconstruction of ODFs or streamlines. This is only a first step: multivariate measures of *dissimilarity* can be applied to local termination patterns or machine learning techniques could be used to classify individuals into groups. Machine

learning approaches will also benefit from LTPA. The feature space in a connectivity-based classification problem scales in dimensionality as a function of the N regions present in the atlas. For a global termination pattern analysis that considers all streamlines (Richiardi et al. 2011), the feature space will span $N(N-1)/2$ dimensions, raising the potential for over-fitting in small datasets. An LTPA search sphere will contain strictly fewer connected regions, effectively acting as an anatomically-based feature selection mechanism. Additionally, we used the simplest connectivity measure possible, streamline count, as our measure of connectivity between region pairs. Count is one of many measures, such as along-track anisotropy, that could be used alternatively.

We propose that a publicly available database of spatially indexed high resolution tractography could be useful in the study of white matter conditions. An exhaustive sphere search is a tool well-suited for exploring neurological conditions where no specific structure is hypothesized to be affected a priori. The same database can be searched with sets of coordinates other than spheres - any region of interest could be uploaded and queried so that termination patterns could be compared across many individuals.

While it is possible that less expensive, lower resolution DWI methods may provide comparable results to DSI-based LTPA, they are also known to fail at reconstructing U-fibers and tracts known to cross. We predict that if LTPA were run on DTI-based tractography then Fig. 3 would resemble Fig. 4: large non-crossing structures would be reproducible but high variability in tractography where the tensor model fails would make U-fibers and crossing tracts unreliable. However, as tractography methods improve (Kreher et al. 2008) and more nuanced ODF models are employed it may become plausible to use low resolution DWI data with LTPA.

Acknowledgments The authors thank Dani Bassett, Mario Mendoza, Philip Beach, Zsuzsi Fodor and Frank Yeh.

References

Basser, P., Pajevic, S., Pierpaoli, C., Duda, J., Aldroubi, A. (2000). In vivo fiber tractography using DT-MRI data. *Magnetic Resonance in Medicine*, *44*(4), 625–632.

Basser, P.J., & Jones, D.K. (2002). Diffusion-tensor MRI: theory, experimental design and data analysis. *NMR in Biomedicine*, *15*, 456–467.

Bassett, D., Brown, J., Deshpande, V., Carlson, J., Grafton, S. (2011). Conserved and variable architecture of human white matter connectivity. *NeuroImage*, *54*(2), 1262–1279.

Bullmore, E., & Bassett, D. (2011). Brain graphs: graphical models of the human brain connectome. *Annual Review of Clinical Psychology*, *7*, 113–140.

Cammoun, L., Gigandet, X., Meskaldji, D., Thiran, J.P., Sporns, O., Do, K.Q., Maeder, P., Meuli, R., Hagmann, P. (2012). Mapping the human connectome at multiple scales with diffusion spectrum MRI. *Journal of Neuroscience Methods*, *203*(2), 386–397.

Chiang, M.C., McMahon, K.L., de Zubicaray, G.I., Martin, N.G., Hickie, I., Toga, A.W., Wright, M.J., Thompson P.M. (2011). Genetics of white matter development: a DTI study of 705 twins and their siblings aged 12 to 29. *NeuroImage*, *54*(3), 2308–2317.

Dale, A.M., Fischl, B., Sereno, M.I. (1999). Cortical surface-based analysis. I. Segmentation and surface reconstruction. *NeuroImage*, *9*(2), 179–194.

Fernandez-Miranda, J.C., Pathak, S., Engh, J., Jarbo, K., Verstynen, T., Yeh, F.C., Wang, Y., Mintz, A., Boada, F., Schneider, W., Friedlander, R (2012). High-definition fiber tractography of the human brain. *Neurosurgery*, *71*(2), 430–453.

Garyfallidis, E., Brett, M., Amirbekian, B., Nguyen, C., Yeh, F.C., Olivetti, E., Halchenko, Y., Nimmo-Smith, I. (2011). Dipy–a novel software library for diffusion MR and tractography. In *17th annual meeting of the organization for human brain mapping*.

Gerhard, S., Daducci, A., Lemkaddem, A., Meuli, R., Thiran, J.P., Hagmann, P. (2011). The connectome viewer toolkit: an open source framework to manage, analyze, and visualize connectomes. *Frontiers in Neuroinformatics*, *5*(3), 1–15.

Geschwind, N., & Kaplan, E. (1962). A human cerebral deconnection syndrome. *Neurology*, *12*, 675–685.

Hagmann, P., Kurant, M., Gigandet, X., Thiran, P., Wedeen, V.J., Meuli, R., Thiran, J.P. (2007). Mapping human whole-brain structural networks with diffusion MRI. *PLoS ONE*, *2*(7), e597.

Hagmann, P., Cammoun, L., Gigandet, X., Meuli, R., Honey, C.J., Wedeen, V.J., Sporns, O. (2008). Mapping the structural core of human cerebral cortex. *PLoS Biology*, *6*(7), e159.

Hagmann, P., Cammoun, L., Gigandet, X., Gerhard, S., Ellen Grant, P., Wedeen, V., Meuli, R., Thiran, J.P., Honey, C.J., Sporns, O. (2010). MR connectomics: principles and challenges. *Journal of Neuroscience Methods*, *194*(1), 34–45.

Jones, D.K., Knösche, T.R., Turner, R. (2013). White matter integrity, fiber count, and other fallacies: the do's and don'ts of diffusion MRI. *NeuroImage*, *73*, 239–254.

Kreher, B.W., Mader, I., Kiselev, V.G. (2008). Gibbs tracking: a novel approach for the reconstruction of neuronal pathways. *Magnetic Resonance in Medicine*, *60*(4), 953–963.

Kriegeskorte, N. (2006). Information-based functional brain mapping. *Proceedings of the National Academy of Sciences*, *103*(10), 3863–3868.

Richiardi, J., Eryilmaz, H., Schwartz, S., Vuilleumier, P. (2011). Decoding brain states from fMRI connectivity graphs. *NeuroImage*, *56*(2), 616–626.

Shi, F., Yap, P.T., Gao, W., Lin, W., Gilmore, J.H., Shen, D. (2012). Altered structural connectivity in neonates at genetic risk for schizophrenia: a combined study using morphological and white matter networks. *NeuroImage*, *62*(3), 1622–1633.

Sporns, O., Tononi, G., Kötter, R. (2005). The human connectome: a structural description of the human brain. *PLoS Computational Biology*, *1*(4), e42.

Tuch, D.S. (2004). Q-ball imaging. *Magnetic Resonance in Medicine*, *52*(6), 1358–1372.

Van Essen, D.C., & Ugurbil, K. (2012). The future of the human connectome. *NeuroImage*, *62*(2), 1299–1310.

Viswanathan, S., Cieslak, M., Grafton, S.T. (2012). On the geometric structure of fMRI searchlight-based information maps. arXiv:1210.6317.

Wang, R., Benner, T., Sorensen, A.G., Wedeen, V.J. (2007). Diffusion toolkit: a software package for diffusion imaging data processing and tractography. *ISMRM*, *15*, 3720–3720.

Wedeen, V.J., Hagmann, P., Tseng, W.Y.I., Reese, T.G., Weisskoff, R.M. (2005). Mapping complex tissue architecture with diffusion

spectrum magnetic resonance imaging. *Magnetic Resonance in Medicine*, *54*(6), 1377–1386.

Yamagata, B., Barnea-Goraly, N., Marzelli, M.J., Park, Y., Hong, D.S., Mimura, M., Reiss, A.L. (2012). White matter aberrations in prepubertal estrogen-naive girls with monosomic turner syndrome. *Cerebral Cortex*, *22*(12), 2761–2768.

Yeh, F.C., Wedeen, V.J., Tseng, W. (2009). Dataset-independent reconstruction of high angular resolution diffusion sampling schemes by generalized q-space imaging. *Proceedings International Society Magazine Resonance*, *17*, 3544.

Yeh, F.C., & Tseng, W. (2011). NTU-90: a high angular resolution brain atlas constructed by *q*-space diffeomorphic reconstruction. *Neuroimage*, *58*(1), 91–99.

Zalesky, A., Fornito, A., Harding, I.H., Cocchi, L., Yücel, M., Pantelis, C., Bullmore, E. (2010). Whole-brain anatomical networks: does the choice of nodes matter? *NeuroImage*, *50*(3), 970–983.